

## Photoinduced Processes in a Dendritic Zn Porphyrin Structure with a Free-Base Porphyrin Core

Lucia Flamigni,<sup>\*,[a]</sup> Anna Maria Talarico,<sup>[a]</sup> Barbara Ventura,<sup>[a]</sup> Chloé Sooambar,<sup>[b]</sup> and Nathalie Solladié<sup>\*,[b]</sup>

**Keywords:** Dendrimers / Energy transfer / Luminescence / Porphyrinoids / Supramolecular chemistry

The photophysical characterization of a nonameric porphyrin assembly made up of a central free-base and eight peripheral zinc porphyrins connected by flexible nucleosidic linkers, and the identification of the photoinduced processes taking place in the array, is reported. Both singlet–singlet and triplet–triplet energy transfer from the peripheral zinc porphyrins to the free-base porphyrin core is detected. The kinetic parameters of singlet–singlet energy transfer are interpreted by assuming the existence of several nonequilibrated conformations in the array due to the flexibility of the linkages. A fast quenching of the donor beyond the time detection limit of the instrument is also hypothesized and assigned to strong interactions between the zinc chromophores in close contact which can give self-quenching phenomena. For the zinc porphyrin triplet excited state, a triplet–triplet annihilation is detected at moderate photon flux as a consequence of multi-

excitation of the same array. Drastic reduction of the photon flux allows us to determine the triplet energy transfer rate from zinc porphyrin to free-base porphyrin, which is the final recipient of the energy collected by the array. The decay of the triplet state of the core free-base porphyrin is prolonged with respect to the model, indicating a shielding effect of the peripheral groups. Complexation experiments with monodentate and didentate bases have been performed in order to gain insight into the spatial arrangement of the zinc porphyrin chromophores and the proposed mechanism of self-quenching. Association of didentate bases increases the rigidity of the multi-porphyrin structure and improves the energy collection ability.

(© Wiley-VCH Verlag GmbH & Co. KGaA, 69451 Weinheim, Germany, 2006)

### Introduction

Natural photosynthesis is triggered by the absorption of photons by a light-harvesting antenna system with a large absorption cross-section, followed by a rapid and efficient transfer of excitation energy to the reaction center. To mimic the natural processes, artificial light-harvesting antennae require a great number of chromophore units that are well organized in space and able to transfer the absorbed energy to one specific site with high efficiency. Porphyrins are ideal candidates for the construction of light-harvesting arrays and, in the past decade, many artificial multi-porphyrin systems have been developed, such as linear or linear-branched arrays,<sup>[1–5]</sup> rings,<sup>[6–8]</sup> windmills,<sup>[9]</sup> dendrimers,<sup>[10,11]</sup> and other assemblies.<sup>[12,13]</sup> Among these, dendritic frameworks appear to be the most promising arrays as they allow site-specific placement of the dye molecules in a three-dimensional hyperbranched treelike fashion, and a good choice of the chromophoric units permit the conveyance of the collected energy toward the central core.

Many dendritic arrays with a variety of linkers have been developed recently.<sup>[10,13]</sup> We present here a study of the photoinduced processes in a dendritic nonameric porphyrin assembly (Scheme 1) made up of a central free-base porphyrin and eight peripheral zinc porphyrins connected in pairs to the core by a flexible nucleosidic linker whose synthesis has been reported recently.<sup>[14]</sup> The structure can be considered a further step in the elaboration of porphyrin-based antennas with respect to a pentaporphyrin previously reported by our groups.<sup>[15]</sup> The eight peripheral zinc porphyrin chromophores can absorb light extensively over the full visible spectrum and the energy stored can be conveyed to the central free-base porphyrin. The study of convenient model compounds, Zn and FBS (Scheme 1), can help in the elucidation of the fundamental steps occurring upon light absorption in the nonaporphyrin FB-Zn<sub>8</sub>, whose photophysical behavior could be strongly influenced by the existence of different conformations due to the flexible linkers. Steady-state and time-resolved spectroscopic methods are used to quantify the energy-transfer processes.

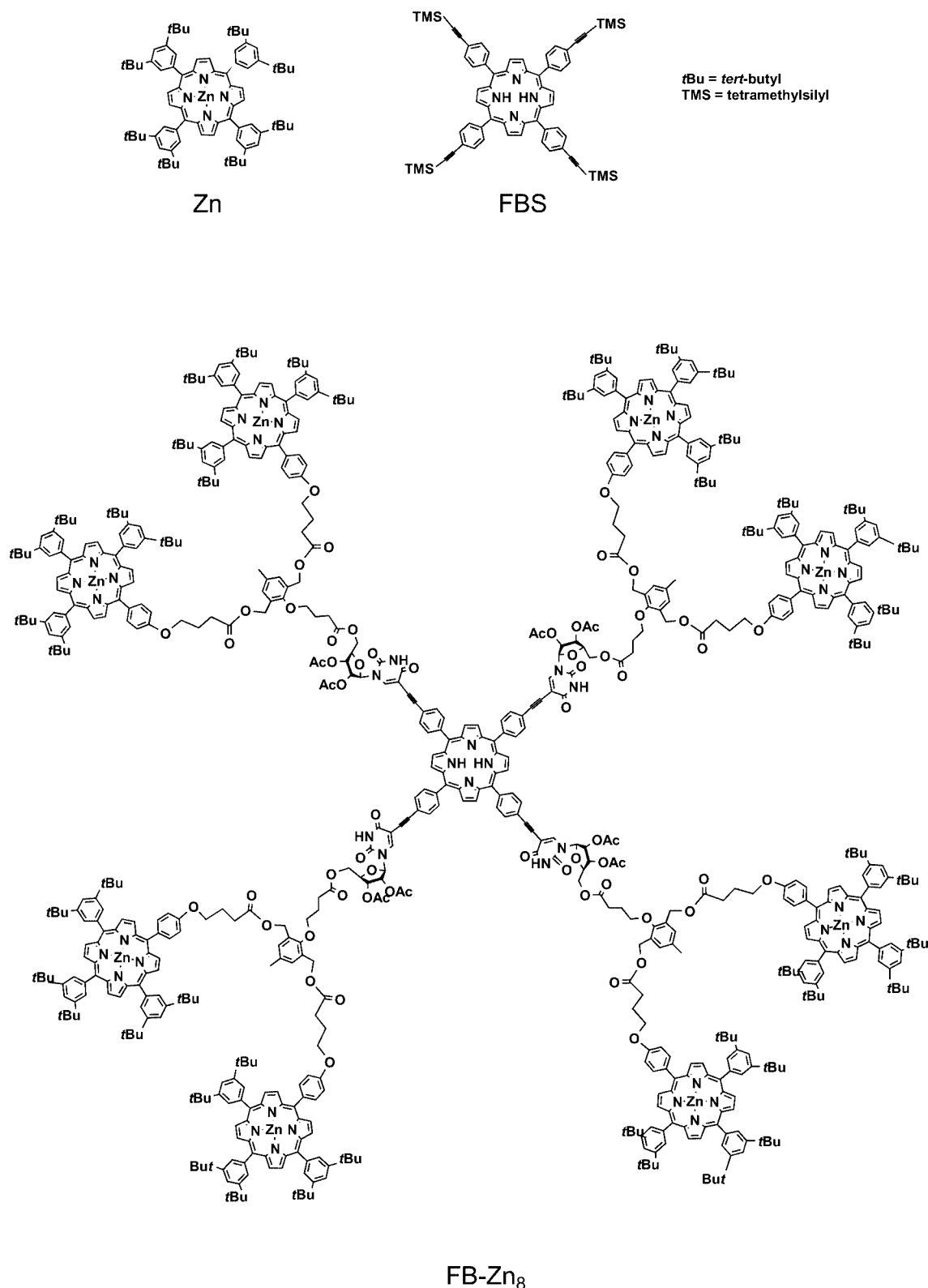
### Results and Discussion

#### Absorption Spectroscopy

Scheme 1 shows the structures of the nonaporphyrin FB-Zn<sub>8</sub> and of the molecules used as models of the periphery

[a] Istituto per la Sintesi Organica e Fotoreattività (ISOF), CNR, Via P. Gobetti 101, 40129 Bologna (Italy)  
Fax: +39-051-639-9844  
E-mail: flamigni@isof.cnr.it

[b] Groupe de Synthèse de Systèmes Porphyriniques (G2SP), Laboratoire de Chimie de Coordination du CNRS (UPR, 8241), 205 route de Narbonne, 31077 Toulouse Cedex 4 (France)  
Fax: +33-5-6155-3003  
E-mail: solladié@lcc-toulouse.fr



Scheme 1. The component models Zn and FBS and the nonaporphyrin FB-Zn<sub>8</sub>.

and the core units, Zn and FBS, respectively. The absorption spectrum of FB-Zn<sub>8</sub> in toluene is in good agreement with the superposition of the model components, as can be seen in Figure 1, where the absorption spectra of the models

are reported with the sum of the nine components and the experimental absorption spectrum of the nonaporphyrin FB-Zn<sub>8</sub>. In addition to the usual broadening of the Soret band, which is typical of covalently bound porphyrinic ar-

rays, a 2–3-nm shift to lower energies can be detected in the maximum wavelength of both the Soret and Q bands with respect to the simple superposition of the components. A long, weak tail extending up to 700 nm can be detected in

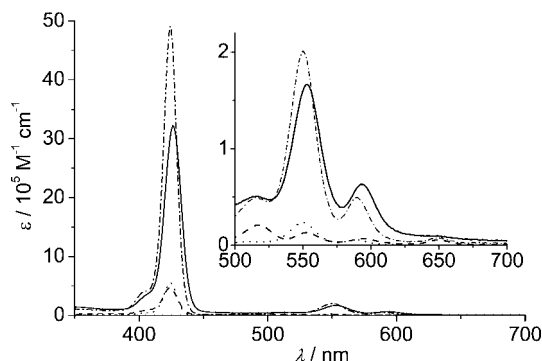


Figure 1. Molar absorption coefficients of the models Zn (dot) and FBS (dash), and of FB-Zn<sub>8</sub> (solid) in toluene solution. The sum of the molar absorption coefficients of the nine components is also reported (dash-dot).

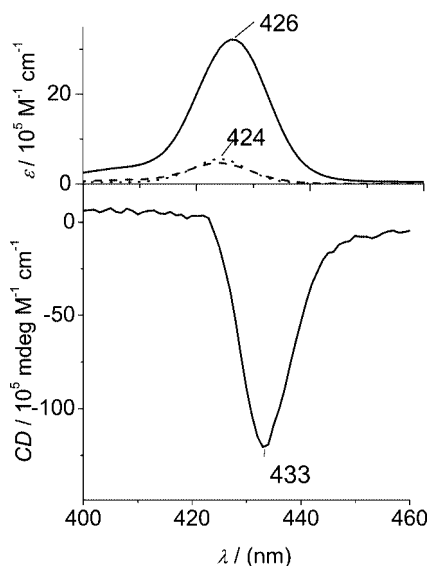


Figure 2. UV (upper panel) and CD (lower panel) spectra of FB-Zn<sub>8</sub> (solid) in toluene solutions. In the upper panel the absorption spectra of components Zn (dot) and FBS (dash) are also reported.

the array compared to the superposition of components, which can be taken as an indication of some interaction between the porphyrinic chromophores. Nonetheless, this interaction is modest and the single chromophores in the array can be considered to retain essentially their own spectroscopic properties (see below).

FB-Zn<sub>8</sub> displays optical activity – the CD spectrum is reported in Figure 2, lower panel, with the absorption spectra of the two models Zn and FBS and the array shown in the upper panel. In the spectrum the positive band is almost absent, whereas a strong, negative band can be detected. Its origin could be assigned to exciton interactions between the porphyrin chromophores, similarly to what was recently reported and discussed in detail for a similar porphyrin pentamer,<sup>[15a]</sup> however, we cannot exclude a CD effect induced on the porphyrin by the chiral nucleosidic linkers.

## Luminescence

The Zn singlet excited state at 295 K in toluene has a lifetime of 2.2 ns and an emission quantum yield of 0.08,<sup>[16]</sup> whereas the lifetime of FBS under the same conditions is 9.5 ns and the emission quantum yield is 0.18. The energy levels of the lowest singlet excited state of the models, derived from the maximum of the emission band at 77 K, are 2.08 eV for <sup>1</sup>Zn and 1.92 eV for <sup>1</sup>FBS (Table 1), which means that a photoinduced energy transfer from the peripheral Zn to the core FBS would spontaneously occur with a  $\Delta G^0$  value of  $-0.16$ . Phosphorescence from porphyrin components could be detected in the near-IR region at 77 K in glassy media.<sup>[17]</sup> From the maximum of the phosphorescence bands, the energy levels of the triplet can be derived for <sup>3</sup>Zn (1.6 eV) and for <sup>3</sup>FBS (1.48; Table 1). An energy transfer could also occur spontaneously in this case from the triplet excited state localized on the zinc porphyrin to the free-base central unit with a  $\Delta G^0$  of  $-0.12$  eV.

The luminescence spectrum of FB-Zn<sub>8</sub> in toluene upon excitation at 550 nm is reported in Figure 3 together with the superposition of the emission spectra of the individual components (Zn and FBS) in toluene, for absorbance corresponding to the same number of photons absorbed by the units in the array. The band positions of the units in the

Table 1. Luminescence properties of the nonaporphyrin and of the models at 295 and 77 K.

	State	295 K				77 K	
		$\lambda_{\max}$ [nm]	$\Phi_{\text{fl}}^{[a]}$	$\Phi_{\text{fl}}^{[b]}$	$\tau$ [ns] <sup>[c]</sup> (% component)	$\lambda_{\max}$ [nm]	$E$ [eV] <sup>[d]</sup>
FBS	<sup>1</sup> FBS	652	0.18	0.08	9.5	646	1.92
	<sup>3</sup> FBS <sup>[e]</sup>					840	1.48
Zn	<sup>1</sup> Zn	594				596	2.08
	<sup>3</sup> Zn <sup>[e]</sup>					776	1.60
FB-Zn <sub>8</sub>	<sup>1</sup> FB-Zn <sub>8</sub>	651	0.10	0.015	9.0 0.175; 0.990; 2.2 (50%; 30%; 20%)	648	1.91
	FB- <sup>1</sup> Zn <sub>8</sub>	600				605	2.05
	<sup>3</sup> FB-Zn <sub>8</sub>					n.d.	
	FB- <sup>3</sup> Zn <sub>8</sub>					n.d.	

[a] FBS Emission quantum yield; selective excitation of the free-base porphyrin unit was at 650 nm. [b] Emission quantum yield, the excitation was at 550 nm; the yield for the array was calculated on the basis of the photons absorbed by the Zn unit. [c] Excitation at 532 nm for lifetimes of less than 1 ns, excitation at 337 nm for lifetimes above 1 ns. [d] Energy levels from the emission maxima at 77 K. [e] Taken from the literature.<sup>[16]</sup>

array are essentially unaltered with respect to the models, thereby confirming that the components retain their own spectroscopic properties. A partial quenching of the zinc porphyrin component ( $\lambda_{\text{max}} = 600 \text{ nm}$ ) to about 20% can be detected, ( $\Phi_{\text{F}} = 0.015$ ) but no corresponding sensitization of the free-base component ( $\lambda_{\text{max}}$  at 651 nm and 720 nm) appears. This observation could be explained by a self-quenching of the zinc porphyrin donors that does not lead to a sensitization of the free-base acceptor and/or to a change in the emissive properties of the free-base core compared to the model FBS. In order to establish whether the present system displays some form of light energy collection and transfer properties, the experiments described below were carried out.

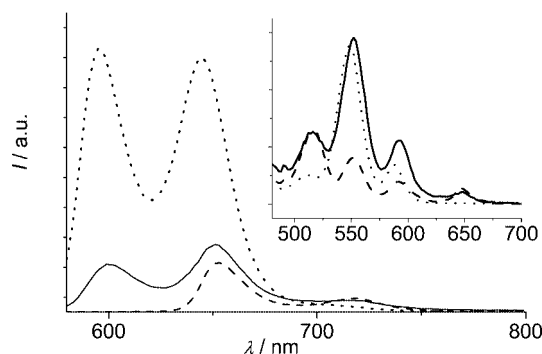
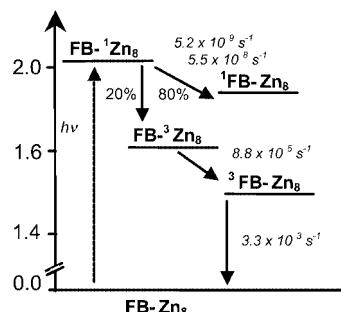


Figure 3. Emission spectra at 295 K of the models Zn (dot), FBS (dash), and of FB-Zn<sub>8</sub> (solid) in toluene solution upon excitation at 550 nm. The concentrations are adjusted to provide the same absorbance of the models and of the corresponding unit in FB-Zn<sub>8</sub>. The inset shows the excitation spectrum registered at  $\lambda_{\text{em}} = 720 \text{ nm}$  for the models and the array.

The emission quantum yield of the porphyrin core in the array was determined by selective excitation of the free-base porphyrin unit at 650 nm and turned out to be reduced ( $\Phi_{\text{F}} \approx 0.10$ <sup>[18]</sup>) with respect to  $\Phi_{\text{F}} = 0.18$  in the model FBS). This perturbation could be the result of interaction of the porphyrin core with some peripheral Zn porphyrin that is in close contact because of the flexibility of the linker. At short distances, low lying charge-transfer states could play a role, leading to a static quenching of the free-base porphyrin. The long absorption tail detected in the nonamer (see above) up to 700 nm could confirm the presence of such an interaction generating low-lying states that are able to quench the free-base porphyrin luminescence. Support in favor of an energy transfer in the array comes from the excitation spectrum detected at  $\lambda_{\text{em}} = 720 \text{ nm}$ , where only the free-base porphyrin core emits (inset of Figure 3). From this spectrum, which is displayed with the excitation spectra of the components, the contribution of the zinc porphyrin unit at 550 nm to the emission of the free base at 720 nm is quite evident, and confirms that an energy transfer from the peripheral components to the core is actually taking place. The fact that there is no evidence of this transfer from the steady-state luminescence experiment as a sensitization of the free-base porphyrin unit (Figure 3) could be ascribed to a decreased emission yield of the energy ac-

ceptor free-base unit from  $\Phi_{\text{F}} = 0.18$  to 0.10, as reported above.

The spectroscopic data from Table 1 allow us to draw a schematic energy-level diagram for FB-Zn<sub>8</sub> (Scheme 2), from which both a singlet-to-singlet (FB-<sup>1</sup>Zn<sub>8</sub> → <sup>1</sup>FB-Zn<sub>8</sub>) and a triplet-to-triplet (FB-<sup>3</sup>Zn<sub>8</sub> → <sup>3</sup>FB-Zn<sub>8</sub>) energy transfer appear feasible.



Scheme 2. Schematic energy-level diagram and photoinduced processes in FB-Zn<sub>8</sub>. The percentage of units following different reaction paths is reported.

### Singlet–Singlet Energy Transfer

The mechanism of singlet–singlet energy transfer between porphyrins is generally of the Förster type,<sup>[19]</sup> with a mechanism involving a dipole–dipole interaction. For this mechanism it is possible to calculate the rate,  $k_{\text{F}}^{\text{F}}$ , as a function of the donor–acceptor distance,  $d_{\text{DA}}$ , with some accuracy as the emission quantum yield,  $\Phi$ , and the lifetime,  $\tau$ , of the donor Zn, the overlap integral,  $J^{\text{F}}$ , and the refractive index of toluene,  $n$ , are known; see Equation (1).<sup>[19]</sup>

$$k_{\text{F}}^{\text{F}} = \frac{8.8 \times 10^{-25} \cdot \kappa^2 \cdot \Phi}{n^4 \cdot \tau \cdot d_{\text{DA}}^6} \cdot J^{\text{F}} \quad (1)$$

$J^{\text{F}}$  is calculated from the experimental emission and absorption spectra to be  $5.47 \times 10^{-14} \text{ cm}^3 \text{ M}^{-1}$  and  $\kappa^2$ , the orientation factor, is taken as 2/3 since the partners can be assumed to randomly approach each other because of the long, flexible linker. On the basis of these parameters and of the data in Table 1, a critical transfer distance,  $R_{\text{c}}$ , which is the distance at which the energy transfer rate equals the intrinsic deactivation rate of the donor, of about 28 Å can be calculated. In view of the approximations involved in the present determinations, we can assume that for a fully extended linkage, corresponding to a center-to-center distance of about 34 Å, essentially no quenching of the donor can occur.<sup>[20]</sup> Due to the flexibility of the linkages, a large number of conformations are expected, characterized by distances varying between a few angstroms, for conformations corresponding to a highly bent linkage, and a maximum distance of 34 Å. The time decay of the luminescence of the zinc porphyrin detected at 600 nm in FB-Zn<sub>8</sub> in toluene (Figure 4) is in perfect agreement with this picture as it displays a multi-exponential decay. This is typical of the luminescence decay of Zn porphyrin donors in either flexible or rigid dendritic multiporphyrin arrays for light har-

vesting and is due to the existence of several donor–acceptor couples with different distances and orientations.<sup>[21]</sup> A three exponential fitting of the zinc porphyrin luminescence decay gives satisfactory results, with *average* calculated lifetimes of 0.175, 0.990, and 2.2 ns with relative weights of 50%, 30%, and 20% respectively. Whereas most of the emission is fitted by lifetimes shorter than that of the reference model Zn, indicating an important quenching, a residual 20% (under our experimental conditions) displays the same lifetime (2.2 ns) as the model. This could be due to the fraction of conformers with donor–acceptor distances corresponding to the fully extended array (34 Å), which are not liable to quenching, although the contribution of zinc porphyrin impurities cannot be excluded. The time profile of the luminescence detected at 720 nm, a wavelength typical of the free-base acceptor, is also shown in Figure 4. Although rather weak, it comes, in fact, from one of the nine chromophores – the luminescence-time evolution in FB-Zn<sub>8</sub> shows a clear rise in the luminescence at early times on the same time scale as the fast decay of the zinc porphyrin donor at 600 nm. A fitting of the formation and decay signal would be meaningless due to the poor signal-to-noise ratio and the multi-exponential nature of the kinetics. The detected formation at 720 nm can be assigned to sensitization of the free-base porphyrin units by the Zn porphyrin moieties. The subsequent time evolution detected at 720 nm can be considered a superposition of the tail of the zinc porphyrin moiety ( $\lambda_{\text{max}} = 600$  nm; lifetime: 2.2 ns) and the decay of the free-base unit emissions ( $\lambda_{\text{max}} = 720$  nm; lifetime: 9 ns).

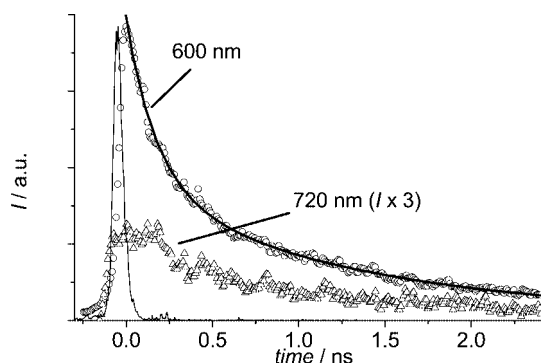


Figure 4. Time-resolved luminescence of FB-Zn<sub>8</sub> in toluene solution after excitation at 532 nm. Decay at 600 nm (circle) is shown with the tri-exponential fitting with lifetimes of 175 ps, 990 and 2.2 ns. The time profile of the luminescence at 720 nm is also reported (triangle) with the exciting flash profile.

It is interesting to compare the steady-state luminescence results with the time-resolved data. The emission quantum yield,  $\Phi_{\text{fl}}$ , is related to the lifetime of a species by the equation  $\Phi_{\text{fl}} = \tau k_{\text{r}}$ , where  $\tau$  is the lifetime and  $k_{\text{r}}$  is the radiative rate constant. In case of more than one lifetimes of the species, as in the present case, where a multi-exponential decay of the luminescence is present, the equation becomes  $\Phi_{\text{fl}} = \sum(f_i \tau_i k_{\text{r}})$ , where  $f_i$  is the fraction of component corresponding to the lifetime  $\tau_i$ . Assuming that  $k_{\text{r}}$  of the zinc porphyrin singlet excited state in FB-Zn<sub>8</sub> is identical to that

of the model Zn ( $k_{\text{r}} = \Phi_{\text{fl}}/\tau$ ;  $k_{\text{r}} = 3.6 \times 10^7 \text{ s}^{-1}$ ) the fluorescence quantum yield can be calculated from the following equation:  $\Phi_{\text{f}} = k_{\text{r}} \times (f_1 \tau_1 + f_2 \tau_2 + f_3 \tau_3)$ , where the index 1, 2, and 3 is relative to the average conformations displaying the three different lifetimes. The result of this calculation is  $\Phi_{\text{f}} = 0.03$ , which is different from the experimental value ( $\Phi_{\text{f}} = 0.015$ ; Table 1). This discrepancy, which is much higher than the experimental uncertainty, could be accounted for by: (i) the radiative rate constant of the zinc porphyrin moiety in the nonaporphyrin is different than the one of the model, and/or (ii) there is some faster quenching, which escapes the time resolution of the experimental set-up (20 ps) and can therefore be considered a “static quenching”. This would be detectable by steady-state techniques, which integrate a signal over time, but *not* by time-resolved methods with time resolution exceeding the timescale of the process. In the latter case, the correct fraction,  $f_i$ , of each component for the calculation of  $\Phi_{\text{f}}$  should be scaled to take into account the component which gives “static” quenching and which is missed by our apparatus.

The luminescence properties at 295 K and 77 K are summarized in Table 1.

### Triplet–Triplet Energy Transfer

Porphyrin triplets exhibit strong and well-characterized triplet absorption spectra and lifetimes in the hundreds of microseconds range in fluid, oxygen-free solutions. They can be conveniently monitored by laser flash photolysis with nanosecond/microsecond resolution. The transient change in the absorption spectra due to the triplet excited states of the models FBS and Zn are reported in Figures 5 and 6, respectively, with one inset (a) showing the lifetime in oxygen-free and the other (b) in air-equilibrated toluene solutions at 295 K. To prevent triplet–triplet second-order competitive reactions, which are a very common phenomenon for long-lived triplet excited states, the lifetime of the species in air-free solutions was measured at extremely low excitation energy ( $\leq 0.2$  mJ per pulse) in order to provide a low concentration of excited species and a good single exponential decay of the excited triplet [insets (a) of Figures 5 and 6]. The triplets are quenched by oxygen and their lifetime in air-saturated solutions is greatly decreased [see Table 2, insets (b) of Figures 5, and 6]. Since the concentration of O<sub>2</sub> in air-equilibrated toluene solutions is  $1.8 \times 10^{-3} \text{ M}$ ,<sup>[22]</sup> a reaction rate with oxygen in toluene of the order of  $1\text{--}1.5 \times 10^9 \text{ M}^{-1} \text{ s}^{-1}$  can be derived for Zn and FBS, in agreement with previous reports.<sup>[23]</sup>

In FB-Zn<sub>8</sub>, once the triplet state of the zinc porphyrin unit is formed, a triplet energy transfer to the core free-base porphyrin can be envisaged. Energy transfer between triplet states occurs generally by a Dexter (electron-exchange) mechanism.<sup>[24]</sup> This type of mechanism involves the synchronized transfer of two electrons, one from the LUMO of the donor to the LUMO of the acceptor and the other from the HOMO of the acceptor to the HOMO of the donor. It requires either a direct physical contact (through



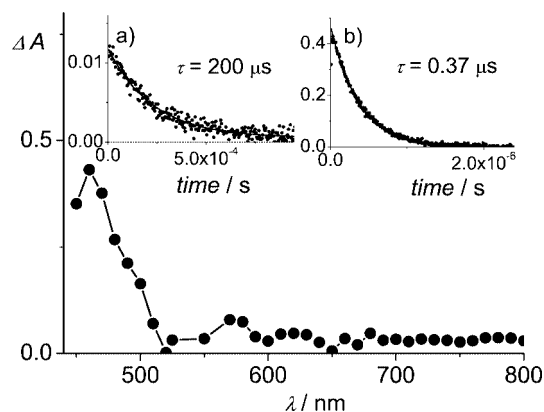


Figure 5. Transient absorbance changes of FBS ( $A = 0.13$ ) following laser excitation at 532 nm (5 mJ per pulse) in toluene solutions. Inset a) shows the decay in oxygen-free (0.2 mJ per pulse) and inset b) the decay in air-saturated solution (5 mJ per pulse).

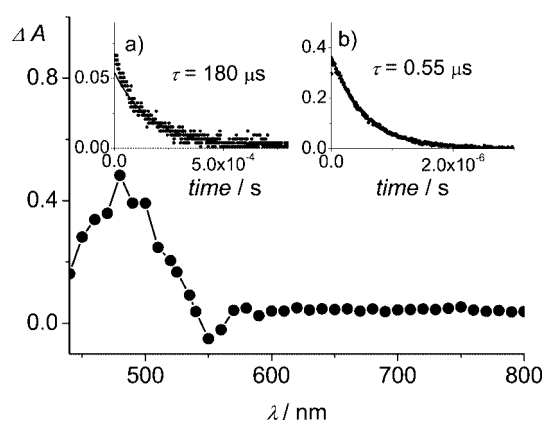


Figure 6. Transient absorbance changes of Zn ( $A = 0.12$ ) following laser excitation at 532 nm (5 mJ per pulse) in toluene solutions. Inset a) shows the decay in oxygen-free (0.125 mJ per pulse) and inset b) the decay in air-saturated solution (5 mJ per pulse).

Table 2. Transient absorbance data at 295 K in toluene.

	State	$\tau$ [ $\mu$ s] <sup>[a]</sup>	$\tau$ [ $\mu$ s] <sup>[b]</sup>	$\Phi_T$ <sup>[c]</sup>
Zn	$^3\text{PZn}$	250	0.50	1
FBS	$^3\text{FBS}$	200	0.37	1
FB-Zn <sub>8</sub>	FB- $^3\text{Zn}_8$	1.1	n.d.	0.2
	$^3\text{FB-Zn}_8$	300	n.d.	ca. 1 <sup>[d]</sup>

[a] Lifetime in air-free toluene, low laser energy (see text). [b] Lifetime in air-saturated toluene. [c] Triplet formation quantum yields, relative to the models and calculated on the basis of the photons absorbed by the unit in the array. [d] Poor signal to noise ratio, the determination is subject to an error of the order of 30%.

space), or the intermediacy of a linkage (through bond), between the reacting partners. Without entering into detail, in the case of through-bond transfer the rate depends on the type of bond and its length. For alkane chains and large distances, as in the present case, the through-bond energy transfer rate is slow and is expected to occur on the micro-

second timescale; it is therefore able to compete with the deactivation rate of the Zn porphyrin triplet in air-free solutions.

A nanosecond flash photolysis experiment on the nona FB-Zn<sub>8</sub> in air-free solution allowed us to detect an end-of-pulse spectrum mostly ascribable to the zinc porphyrin triplet state (Figure 7). The yield of formation of this state calculated with respect to the model Zn in the wavelength range out of the ground-state absorbance (650–700 nm) is about 20%, which is in good agreement with the fraction of unquenched singlet derived by luminescence time-resolved determinations (see above). This clearly indicates that the triplet states are produced only by the unquenched singlet excited states of the zinc porphyrin donor via an intersystem-crossing step. The end-of-pulse spectrum of FB-Zn<sub>8</sub> evolves rapidly, with a slight shift of the maximum from 490 to 480 nm, and after a few microseconds it reaches a value that is stable on the microsecond timescale (Figure 7). The exponential decay rate of the fast decay was found to depend on the laser intensity, as shown in inset (a) of Figure 7. This can be understood by considering that excitation of a  $3 \times 10^{-6}$  M solution with several millijoules at 532 nm is able to produce multiple excitation of porphyrins (mostly of the zinc porphyrin units, which absorb 85% of the incident photons) within the same array.<sup>[25]</sup> Multiple excitation in an array that has a very high *local* concentration of zinc porphyrins would cause a fast intramolecular triplet–triplet reaction and lead to a rapid self-quenching of the zinc porphyrin triplet. The experimental first-order reaction rate would therefore be due to the contribution of two different processes: the intramolecular triplet–triplet annihilation, which is dependent on the square of the laser energy, and the energy-transfer process, which is independent of it. The rate at different incident laser conditions was measured and a plot of rate versus laser intensity was extrapolated to zero energy [inset (a) of Figure 7] in order to derive the decay rate of FB- $^3\text{Zn}_8$  in the absence of multi-photon excitation. Under these conditions, the first-order decay rate of FB- $^3\text{Zn}_8$  was  $8.8 \times 10^5 \text{ s}^{-1}$  and was assigned to an energy-transfer process from the triplet localized on the zinc porphyrin moiety (FB- $^3\text{Zn}_8$ ) to the triplet localized on the free-base central unit ( $^3\text{FB-Zn}_8$ ).<sup>[26]</sup> The latter species, which can be identified from the spectrum after 3  $\mu$ s in Figure 7, decays exponentially with a lifetime of 300  $\mu$ s [inset (b) of Figure 7]. The lifetime of the triplet porphyrin core in  $^3\text{FB-Zn}_8$  is longer than that determined for the model FBS under the same conditions (ca. 200  $\mu$ s), very likely because of a sort of shielding effect of the periphery components toward traces of oxygen or quenching contaminants in the solution. A similar protecting effect of the periphery on the triplet excited state of a core chromophore was previously found for a similar pentaporphyrin<sup>[15]</sup> and has also been reported for a fullerene-based dendrimeric structure.<sup>[27]</sup>

Scheme 2 shows the rate constants of the intramolecular processes; the decay of the excited state localized on the zinc porphyrin chromophore, FB- $^1\text{Zn}_8$ , is assigned to different processes depending on the type of conformation: the 20% extended conformation decays mainly to the triplet state

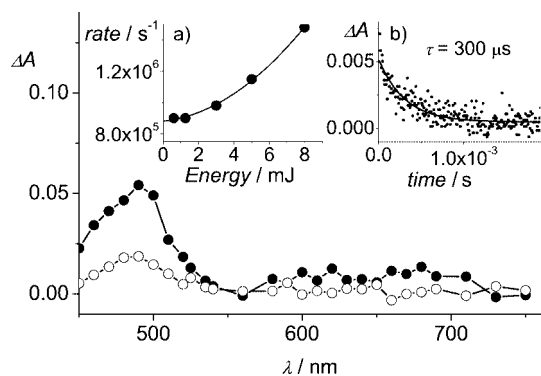


Figure 7. Transient absorbance changes of FB-Zn<sub>8</sub> ( $A = 0.17$ ) following laser excitation at 532 nm (5 mJ per pulse) in toluene solutions; end-of-pulse spectra (filled circle) and 3  $\mu$ s after the end of the pulse (open circle). Inset a) shows the rate constant dependence of the fast decay (see text) from the laser intensity and inset b) shows the decay of the 3- $\mu$ s species, assigned to <sup>3</sup>FB-Zn<sub>8</sub>, in oxygen-free solutions.

FB-<sup>3</sup>Zn<sub>8</sub>, whereas the other conformations with lower donor–acceptor distances decay by energy transfer to <sup>1</sup>FB-Zn<sub>8</sub> with average rates of  $5.2 \times 10^9$  and  $5.5 \times 10^8$  s<sup>−1</sup>, corresponding respectively to average lifetimes of 175 and 990 ps.

### Complexation

Zinc porphyrins are known to axially bind pyridine or pyridyl residues with association constants of the order of  $10^4$  M<sup>−1</sup>. These constants have been found to increase dramatically up to around  $10^6$  to  $10^8$  M<sup>−1</sup> when multiple bonds can contribute to the formation of the complex.<sup>[28,29]</sup>

We have undertaken this type of experiment with both monodentate pyridine (Pyr) and didentate 4,4'-bipyridine (Bipy) in order to gain information about the spatial arrangement and the interactions between the zinc porphyrin chromophores in FB-Zn<sub>8</sub>. As a reference, the same experiments were performed with Zn. Our aim was to derive the association constants by spectrophotometric and spectrofluorimetric methods and to monitor the effect of FB-Zn<sub>8</sub> complexation on CD spectroscopy, in order to gain some insight into the system. The association constants were derived by a nonlinear treatment previously developed for the analysis of absorption and emission signals at a selected wavelength (see Exp. Sect. for details).<sup>[29]</sup>

The results for the absorption of Zn ( $1.7 \times 10^{-6}$  M) upon titration with increasing amounts of Pyr are reported in Figure 8, together with the emission spectra of the same solutions upon excitation at 428 nm, which is the isosbestic point between the complexed and uncomplexed forms. The insets show the nonlinear fittings to the experimental data, and the derived association constants are summarized in Table 3. The same type of experiment was also performed with Bipy as a titration agent, and the results are illustrated in Figure 9. The plots of the signals at the selected wavelengths (inset) allow us to derive the association constants (Table 3). The behavior with the two different titration agents is essentially the same for Zn: in both cases the ab-

sorption of the porphyrin Soret band shifts from 424 to 431 nm (7 nm), with a clear isosbestic at 428 nm typical of the formation of a 1:1 complex.<sup>[30]</sup> In principle, the didentate Bipy could complex two Zn molecules to form a 2:1 (Zn/Bipy) complex, which should be favored at low concentrations of Bipy. Nonetheless, in the present experimental conditions we were unable to detect the 2:1 complex, which is reported to display a red shift of only about 4 nm with respect to the Zn porphyrin band, i.e. a band maximum at lower wavelengths with respect to the 1:1 complex.<sup>[30]</sup> The low association constant and the use of a large excess of Bipy are very likely to be unfavorable for the formation of the 2:1 complex.

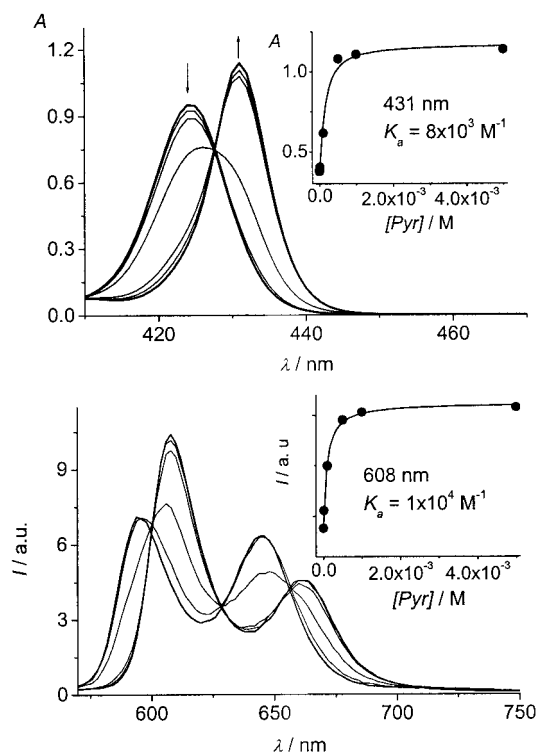


Figure 8. Zn ( $1.7 \times 10^{-6}$  M) in toluene solution upon titration with increasing amounts of Pyr. The upper panel shows the change of absorbance in the Soret band region and the inset shows the data points at 431 nm, fitted according to Equation (2). In the lower panel the change in emission intensity is shown and in the inset the data points at 608 nm, fitted to Equation (2), are reported.

Table 3. Association constants  $K_a$  [M<sup>−1</sup>] of the model Zn and of FB-Zn<sub>8</sub> with pyridine and bipyridine.

	Pyr		Bipy			
	Abs	Em	Average Abs	Average Em	Average Abs	Average Em
Zn	$8 \times 10^3$	$1 \times 10^4$	$9 \times 10^3$	$9 \times 10^3$	$1.4 \times 10^4$	$1.2 \times 10^4$
FB-Zn <sub>8</sub>	$6 \times 10^3$	$6 \times 10^3$	$6 \times 10^3$	—	—	—

In the case of titration of a solution of FB-Zn<sub>8</sub> ( $2.6 \times 10^{-7}$  M), the results obtained with Pyr and Bipy are rather different. The effects on the absorption and emission properties upon titration with the monodentate Pyr are shown in Figure 10. The absorption titration data do not differ appreciably from that of the model Zn – the shift in

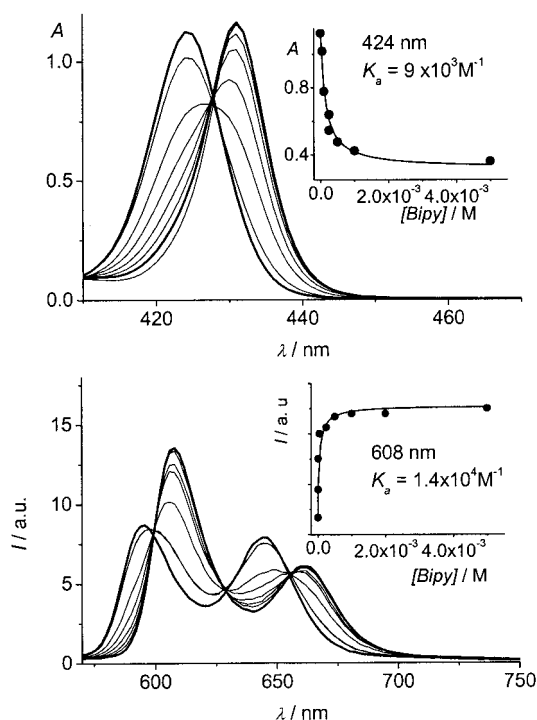


Figure 9. Zn ( $1.7 \times 10^{-6}$  M) in toluene solution upon titration with increasing amounts of Bipy. The upper panel shows the change of absorbance in the Soret band region and the inset shows the data points at 424 nm, fitted according to Equation (2). In the lower panel the change in emission intensity is shown and in the inset the data points at 608 nm, fitted to Equation (2), are reported.

the Soret band of the zinc porphyrin unit upon complexation is from 426 to 431 nm, with a single isosbestic point at 428 nm. The emission data, making allowance for the bands of the free-base unit in FB-Zn<sub>8</sub>, do not appear different from the titration results of the model Zn in the region 570–640 nm, where only the zinc porphyrin chromophore emits. The derived association constant is slightly lower than that determined for the model Zn, and this is perhaps related to the less accessible Zn porphyrin units in the nona structure compared to simple Zn.

The results of titration of FB-Zn<sub>8</sub> with the didentate Bipy are more interesting. Absorption data show that in this case there is no isosbestic point (see Figure 11), but from the initial spectrum of the free nonaporphyrin ( $\lambda_{\max} = 426$  nm) a rather complicated evolution can be detected. This shows an initial decrease of the band at 426 nm with a shift to 429 nm in the concentration range from  $5 \times 10^{-7}$  to  $5 \times 10^{-6}$  M, followed by an increase of the band at 429 nm, which reaches a maximum for a Bipy concentration of  $10^{-4}$  M, and a final evolution for concentrations above  $5 \times 10^{-3}$  M to the absorption with maximum at 431 nm typical of the 1:1 complex spectrum, in analogy to the model system. An absorption maximum around 429 nm is typical of the 2:1 (Zn/Bipy) complex spectrum, but the exact position of the maximum and the extinction coefficient of the species could change slightly depending on the geometry and conformations of the complex. Similar data have recently been reported by Hunter and Ballester.<sup>[31]</sup> In one of

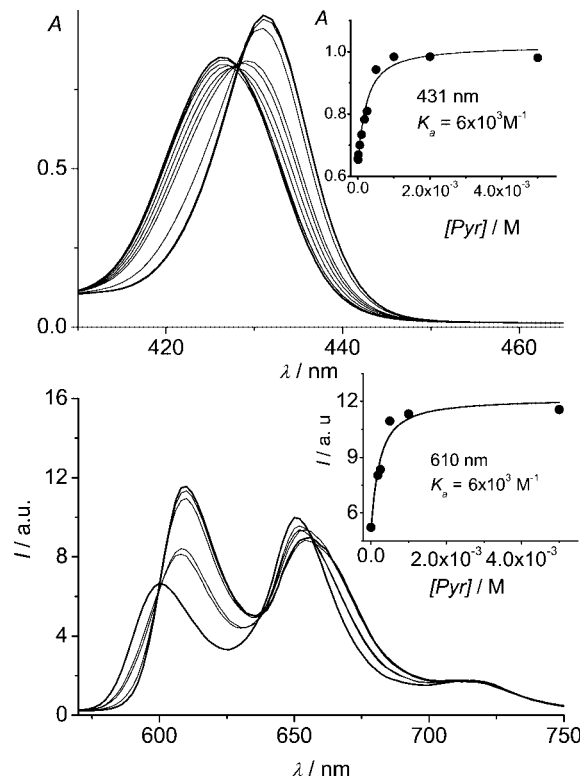


Figure 10. FB-Zn<sub>8</sub> ( $2.6 \times 10^{-7}$  M) in toluene solution upon titration with increasing amounts of Pyr. The upper panel shows the change of absorbance in the Soret band region and the inset shows the data points at 431 nm, fitted according to Equation (2). In the lower panel the change in the emission intensity is shown and in the inset the data points at 610 nm, fitted to Equation (2), are reported.

the cases studied – a calixa-tetraporphyrin titrated by didentate DABCO – they detected a similar behavior in the middle part of the titration by absorption spectroscopy. That behavior was assigned, and confirmed by <sup>1</sup>H NMR spectroscopy, to the formation of a 2:1 complex (Zn/DABCO) with different conformations and geometries. Whereas in Hunter and Ballester's case the presence of different conformations was mainly ascribed to the possibility of formation of intra- or intermolecular complexes, in the present experiment the possibility of forming different 2:1 complexes depends on the relative positions of the porphyrins involved, i.e. whether they are on the same branch or on different branches. We also expect that, due to the high flexibility of the system, the geometry of the complexes could be extremely variable.

The situation is obviously rather complex, and we can only derive from the present data the information that an intermediate group of slightly different 2:1 complexes is formed prior to the formation of a 1:1 complex, which is favored in conditions of high concentration of Bipy. The determination of one or more association constants for this system is far too complex and beyond the purposes of the present work.

Due to the absence of a clear isosbestic point in the absorption experiment it was not possible to perform a neat luminescence titration experiment, as done in the previous



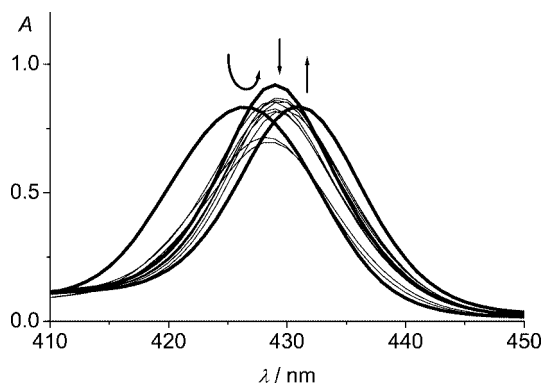


Figure 11. FB-Zn<sub>8</sub> ( $2.6 \times 10^{-7}$  M) in toluene solution upon titration with increasing amounts of Bipy (range  $5 \times 10^{-7}$ – $5 \times 10^{-2}$  M).

cases. It was, however, possible to select some concentrations of titrant and to compare the luminescence of the complex to the luminescence of FB-Zn<sub>8</sub> alone, upon excitation at the iso-absorbing wavelength for the couple of solutions. The data are reported in Figure 12 and seem to indicate that an increase of the luminescence of the zinc porphyrin at 610 nm and of the free-base moiety around 715 nm occurs in FB-Zn<sub>8</sub> upon increasing the complexation degree. In fact, comparing the results of Figure 12 with those of Figure 9, which shows data for the model Zn and Bipy, the band at 610 nm, due to the complexed zinc porphyrin component, appears to be higher in the system FB-Zn<sub>8</sub> plus Bipy than in the model complex Zn plus Bipy (2.4 vs. 1.6). This finding, which is ascribable to a disruption of the interaction between zinc porphyrin chromophores by Bipy, could make available more excitation energy of the zinc porphyrin donor for the energy-transfer process. This type of behavior does not seem to take place for the system FB-Zn<sub>8</sub> plus Pyr (see Figure 10); the difference in the two systems could very likely be due to the larger dimensions and to the didentate binding by Bipy.

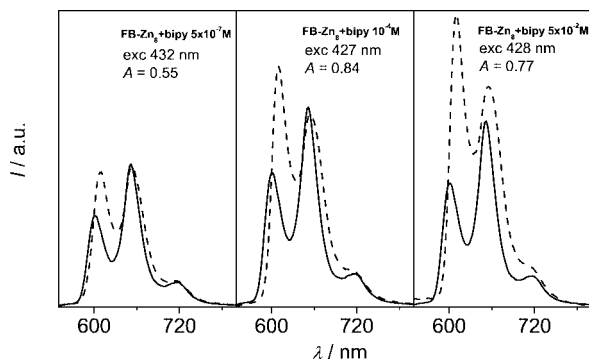


Figure 12. Luminescence spectra of FB-Zn<sub>8</sub> ( $2.6 \times 10^{-7}$  M) in toluene solutions upon different Bipy additions compared to the luminescence of FB-Zn<sub>8</sub> alone. The excitation wavelength corresponds to the iso-absorbing wavelength for each pair of solutions (see text for details).

What is worth noting is the effect that complexation by both Pyr and Bipy has on the CD signal, as shown in Figure 13. It can be seen that complexation is effective in decreasing the optical activity. The CD signal is, however,

not fully cancelled by complexation, as can be seen in the upper panel of Figure 13, where about 40% of the original signal remains at concentrations of Pyr corresponding to complexation of the zinc porphyrin units of 95%.<sup>[32]</sup> Similar results are obtained for the titration with Bipy (lower panel of Figure 13). These data indicate that a nearly complete association of the array with Pyr and Bipy (the completeness of the complexation reaction in the Bipy case can be derived from the invariance of the absorption spectra upon further addition of Bipy) can decrease most of the CD activity but not completely suppress it. Complexation can certainly interfere with exciton coupling by changing the geometry and/or the distance between interacting porphyrins but can also increase the rigidity and influence the geometry of the structure affecting the CD activity induced by chiral nucleosidic linkers. So this does not help to provide a clear identification of the origin of the observed CD effect.

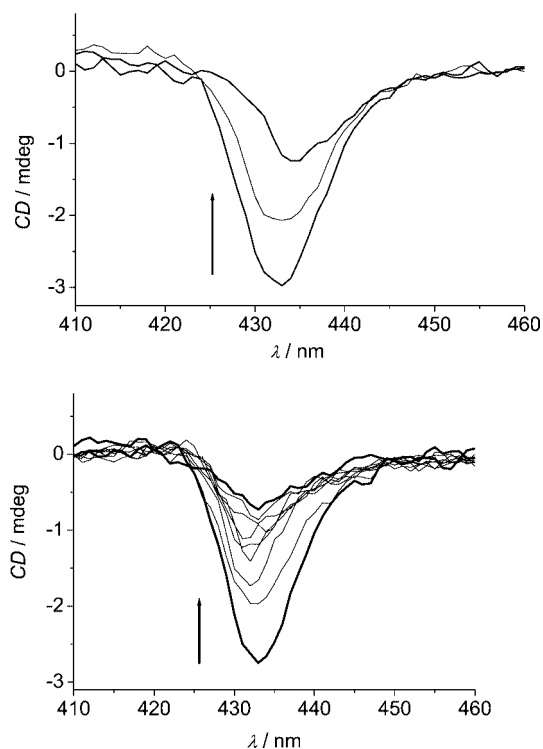


Figure 13. CD spectra of FB-Zn<sub>8</sub> in toluene solutions upon Pyr (upper panel; [Pyr] range  $0$ – $10^{-3}$  M) and Bipy complexation (lower panel; [Bipy] range  $0$ – $5 \times 10^{-2}$  M).

## Conclusions

A full spectroscopic characterization of FB-Zn<sub>8</sub> and of the photoinduced processes in this nonaporphyrin have been performed; singlet–singlet and triplet–triplet energy-transfer processes have been detected and their kinetic parameters derived. Complexation experiments with monodentate Pyr and didentate Bipy have been performed and the association constants have been derived; furthermore, the effect of complexation on the luminescence and on the optical activity have been monitored.

Light absorption of this nonaporphyrin structure appears rather promising for possible applications in solar-energy conversion devices; the molar absorption coefficient has, in fact, extremely high values throughout the visible region with a maximum on the Soret band higher than  $3000000 \text{ M}^{-1} \text{ cm}^{-1}$ . Nonetheless, its performance with respect to the ability to convey the collected light energy to the focal free-base porphyrin seems to be less satisfactory, and transfer to the core free-base porphyrin is not complete in spite of the fact that the quenching of the donor is, for most of the conformations, rather fast. The fact that the absorbed energy is not completely conveyed to the core energy acceptor and/or is not released by the latter as emitted light could be due to interactions between the chromophores, which can come into close contact because of the flexibility of the linkers and bring about self-quenching phenomena. Disruption of the interactions by using some coordinating component to separate the chromophores appears to be a promising strategy to try to overcome/reduce the undesired interactions with a consequent increase of the energy available for the transfer to the core free-base porphyrin acceptor.

## Experimental Section

The synthesis of the nonaporphyrin has been reported elsewhere.<sup>[15]</sup>

**Spectroscopic and Photophysical Determinations:** The solvent used was spectroscopic grade toluene (C. Erba). Absorption spectra were recorded with a Perkin–Elmer Lambda 9 spectrophotometer and emission spectra, uncorrected if not otherwise specified, were recorded with a Spex Fluorolog II spectrofluorimeter equipped with a Hamamatsu R928 photomultiplier. Relative luminescence intensities were evaluated from the area (on an energy scale) of the luminescence spectra corrected for the photomultiplier response. Luminescence quantum yields,  $\Phi$ , for the components were obtained with reference to a standard, namely (1,5,10,15-tetra-*tert*-butylphenyl)porphyrinatozinc(II), in toluene with  $\Phi = 0.08$ .<sup>[16]</sup> Experiments at 77 K made use of quartz capillary tubes immersed in liquid nitrogen contained in a home-made quartz dewar. Circular dichroism spectra were obtained with a Jasco J-710 dichrograph.

Titration experiments for the determination of the association constants were performed using a constant concentration of porphyrins and variable concentrations of Pyr or Bipy. In titration experiments excitation was performed at the isosbestic point of the complexed and uncomplexed porphyrin spectra. Equation (2) was used to derive the association constant,  $K_a$ , where  $K_a$  is  $1/K_d$ ,  $Obs$  is any observable (i.e. absorbance or emission intensity),  $S_0$  is the constant concentration of FB-Zn<sub>8</sub>,  $X$  is the variable concentration of the complexing agent,  $\Delta Obs$  is the maximum variation of the observable under examination and  $Obs_0$  is its value at zero concentration of titration agent.<sup>[28,29]</sup>

$$Obs = Obs_0 + \frac{\Delta Obs}{2S_0} \cdot \{K_d + X + S_0 - [(K_d + X + S_0)^2 - 4XS_0]^{1/2}\} \quad (2)$$

Fluorescence lifetimes in the nanosecond range were detected by an IBH Time-Correlated Single Photon Counting apparatus with excitation at 337 nm. Luminescence lifetimes shorter than one nanosecond were determined by an apparatus based on a Nd:YAG

laser (Continuum PY62-10) with a 35-ps pulse duration (532 nm, 1 mJ per pulse) and a Streak Camera (Hamamatsu C1587 equipped with M1952). The luminescence signals from 1000 laser shots were averaged and the time profile was measured from the streak image in a wavelength range of about 20 nm around the selected wavelength. The fitting of the luminescence decays was performed by standard iterative nonlinear programs taking into consideration the instrumental response.<sup>[33a]</sup> Transient absorbance in the nanosecond range made use of a laser flash photolysis apparatus based on a Nd:YAG laser (JK Lasers) delivering 532-nm pulses of 18 ns. Absorbance of the solutions at the exciting wavelength was about 0.2 and the energy used was 5 mJ per pulse for the determination of the spectra and less than 0.2 mJ per pulse for the triplet lifetime determination, in order to prevent undesired second-order T-T annihilation reactions. Relative triplet yields were calculated with respect to the photons absorbed only by the unit of interest, calculated on the basis of the photon partition in the array, and were determined by comparing the transient absorbance in the region 600–650 nm with that of Zn for FB-<sup>3</sup>Zn<sub>8</sub> and at 680–700 nm with that of FBS for <sup>3</sup>FB-Zn<sub>8</sub>. Experiments on triplets were conducted in homemade, 10-mm optical path cuvettes, bubbled with argon for 5 min, if not otherwise specified. Further details on the experimental setup can be found elsewhere.<sup>[33b,33c]</sup>

Computation of the integral overlap and of the rate of the energy-transfer processes according to the Förster mechanism was performed with Matlab 5.2.<sup>[34]</sup>

Estimated errors are 20% for quantum yields, 30% for association constants, and 10% for lifetimes; the working temperature, if not otherwise specified, was  $295 \pm 2 \text{ K}$ . The error in lifetime determinations is increased in case of multi-exponential fitting to 20%.

## Acknowledgments

Funds from the Italian CNR (project PM-P04-ISTM-C1/ISOF-M5: Molecular, supramolecular and macromolecular components with photonic and optoelectronic properties) and from the Ministero dell'Istruzione, dell'Università e della Ricerca (FIRB, RBNE019H9K) are acknowledged.

- [1] D. Kim, A. Osuka, *J. Phys. Chem. A* **2003**, *107*, 8791–8816.
- [2] N. Atratani, A. Osuka, H. S. Cho, D. Kim, *J. Photochem. Photobiol. C: Photochem. Rev.* **2002**, *3*, 25–52.
- [3] E. Hindin, R. A. Forties, R. S. Loewe, A. Ambroise, C. Kirmayer, D. F. Bocian, J. S. Lindsey, D. Holten, R. S. Knox, *J. Phys. Chem. B* **2004**, *108*, 12821–12832.
- [4] D. Holten, D. F. Bocian, J. S. Lindsey, *Acc. Chem. Res.* **2002**, *35*, 57–69.
- [5] D. Furutsu, A. Satake, Y. Kobuke, *Inorg. Chem.* **2005**, *44*, 4460–4462.
- [6] Y. Nakamura, I.-W. Hwang, N. Aratani, T. K. Ahn, D. M. Ko, A. Takagi, T. Kawai, T. Matsumoto, D. Kim, A. Osuka, *J. Am. Chem. Soc.* **2005**, *127*, 236–246.
- [7] I.-W. Hwang, D. M. Ko, T. K. Ahn, Z. S. Yoon, D. Kim, X. Peng, N. Aratani, A. Osuka, *J. Phys. Chem. B* **2005**, *109*, 8643–8651.
- [8] I.-W. Hwang, M. Park, T. K. Ahn, Z. S. Yoon, D. M. Ko, D. Kim, F. Ito, Y. Ishibashi, S. R. Khan, Y. Nagasawa, H. Miyasaka, C. Ikeda, R. Takahashi, K. Ogawa, A. Satake, Y. Kobuke, *Chem. Eur. J.* **2005**, *11*, 3753–3761.
- [9] A. Nakano, A. Osuka, T. Yamazaki, Y. Nishimura, S. Akimoto, I. Yamazaki, A. Itaya, M. Murakami, H. Miyasaka, *Chem. Eur. J.* **2001**, *7*, 3134–3151.
- [10] Himahori, *J. Phys. Chem. B* **2004**, *108*, 6130–6143 and references cited therein.

- [11] M.-S. Choi, T. Aida, T. Yamazaki, I. Yamazaki, *Chem. Eur. J.* **2002**, *8*, 2668–2678.
- [12] K. Sasaki, K. Sugou, K. Miyamoto, J. Hirai, S. Tsubouchi, H. Miyasaka, A. Itaya, Y. Kuroda, *Org. Biomol. Chem.* **2004**, *2*, 2852–2860.
- [13] a) A. Satake, Y. Kobuke, *Tetrahedron* **2005**, *61*, 13–41; b) A. Morandeira, E. Vauthey, A. Schuway, A. Gossauer, *J. Phys. Chem. A* **2004**, *108*, 5741–5751; c) J. Davila, A. Harriman, L. R. Milgrom, *Chem. Phys. Lett.* **1987**, *136*, 427–430; d) M.-S. Choi, T. Yamazaki, I. Yamazaki, T. Aida, *Angew. Chem. Int. Ed.* **2004**, *43*, 150–158.
- [14] N. Solladié, C. Sooambar, H. Herschbach, J.-M. Strub, E. Leize, A. Van Dorsselaer, A. M. Talarico, B. Ventura, L. Flamigni, *New J. Chem.* **2005**, *29*, 0000–0000.
- [15] a) L. Flamigni, A. M. Talarico, B. Ventura, G. Marconi, C. Sooambar, N. Solladié, *Eur. J. Inorg. Chem.* **2004**, 2557–2569; b) N. Solladié, M. Gross, J.-P. Gisselbrecht, C. Sooambar, *Chem. Commun.* **2001**, 2206–2207.
- [16] M. Dixon, J. P. Collin, J. P. Sauvage, L. Flamigni, *Inorg. Chem.* **2001**, *40*, 5507–5517.
- [17] L. Flamigni, N. Armaroli, F. Barigelletti, V. Balzani, J. P. Collin, J. O. Dalbavie, V. Heitz, J. P. Sauvage, *J. Phys. Chem.* **1997**, *101*, 5936–5943.
- [18] The emission quantum yield of FBS may be affected by an error of about 30%. This is caused by the low absorbance value ( $<0.1$ ) of the unit in the array at the excitation wavelength (650 nm) because of the presence of one FBS unit out of eight Zn porphyrin units.
- [19] Th. Förster, *Discuss. Faraday Soc.* **1959**, *27*, 7–17.
- [20] Distance calculated with CS Chem. 3D Ultra CambridgeSoft. Com., 2000 Cambridge, MA, USA. The calculated quenching at a distance of 34 Å is about 20%. A lifetime reduction of this order can hardly be detected in our experimental conditions, where a multi-exponential fit of the decay, characterized by a large uncertainty, is involved.
- [21] See, for example: A. Nakano, A. Osuka, I. Yamazaki, T. Yamazaki, Y. Nishimura, *Angew. Chem. Int. Ed.* **1998**, *37*, 3023–3027.
- [22] S. L. Murov, I. Carmichael and G. L. Hugh, *Handbook of Photochemistry*, Marcel Dekker, New York, **1993**, p. 293.
- [23] L. Flamigni, A. M. Talarico, M. J. Gunter, M. R. Johnston, T. P. Jaynes, *New J. Chem.* **2003**, *27*, 551–559.
- [24] D. L. Dexter, *J. Chem. Phys.* **1953**, *21*, 836–850.
- [25] 5 mJ at 532 nm correspond to  $1.3 \times 10^{16}$  photons, the analyzed volume (0.04 mL) contains  $8 \times 10^{13}$  units of array. The absorbed photons in the analyzed volume are 7.5%, i.e.  $1.0 \times 10^{15}$  and this can clearly lead to multiple excitation of the same array.
- [26] In order to derive the decay rate of FB-<sup>3</sup>Zn<sub>8</sub>, the following equation was used:  $k_{\text{obs}} = k_{\text{en}} + C \cdot I^2$ , where  $I$  is the laser intensity,  $C$  is a constant,  $k_{\text{obs}}$  is the first-order rate constant observed for the decay of FB-<sup>3</sup>Zn<sub>8</sub> and  $k_{\text{en}}$  is the energy transfer reaction rate.  $k_{\text{en}}$  was derived by extrapolation of the observed rate  $k_{\text{obs}}$  to zero laser intensity.
- [27] J. F. Nierengarten, N. Armaroli, G. Accorsi, Y. Rio, J. F. Eckert, *Chem. Eur. J.* **2003**, *9*, 36.
- [28] a) L. Flamigni, A. M. Talarico, F. Barigelletti, M. R. Johnston, *Photochem. Photobiol. Sci.* **2002**, *1*, 190–197 and references cited therein; b) E. Iengo, E. Zangrando, E. Alessio, J.-C. Chambron, V. Heitz, L. Flamigni, J.-P. Sauvage, *Chem. Eur. J.* **2003**, *9*, 5879–5887 and references cited therein.
- [29] L. Flamigni, A. M. Talarico, B. Ventura, *J. Porphyrins Phthalocyanines* **2003**, *7*, 317–326.
- [30] C. C. Mak, N. Bampos, J. K. M. Sanders, *Angew. Chem.* **1998**, *110*, 3169–3172; *Angew. Chem. Int. Ed.* **1998**, *37*, 3020–3023.
- [31] a) L. Baldini, P. Ballester, A. Casnati, R. M. Gomila, C. A. Hunter, F. Sansone, R. Ungaro, *J. Am. Chem. Soc.* **2003**, *125*, 14181–14189; b) P. Ballester, A. Costa, A. M. Castilla, P. M. Deyà, A. Frontera, R. M. Gomila, C. H. Hunter, *Chem. Eur. J.* **2005**, *11*, 2196–2206.
- [32] The fraction of complexation,  $f$ , can be determined by the following equation:  $f = 1 - [1/(1 + [\text{Pyr}] K_a)]$ .
- [33] a) L. Flamigni, *J. Phys. Chem.* **1993**, *97*, 9566–9572; b) L. Flamigni, *J. Phys. Chem.* **1992**, *96*, 3331–3337; c) L. Flamigni, *J. Chem. Soc., Faraday Trans.* **1994**, *90*, 2331–2336.
- [34] *Matlab* 5.2. The MathWorks Inc. Natick Ma 01760, USA.

Received: November 21, 2005  
Published Online: March 30, 2006